

Supplementary information for

Surface Fluoride Management for Enhanced Stability and Efficiency of Halide Perovskite Solar Cells via Thermal Evaporation Method

Wei-Min Gu, Yue Zhang, Ke-Jian Jiang*, Guanghui Yu, Yanting Xu, Jin-Hua Huang, Yanyan Zhang, Fuyi Wang, Yawen Li, Yuze Lin, Xinning Jiao, Cai-Yan Gao, Haochen Fan, Ningning Wu, Xueqin Zhou, Yanlin Song*

*Corresponding author. Email: kjjiang@iccas.ac.cn (K.-J.J.);
ylsong@iccas.ac.cn (Y.S.).

This PDF file includes:

Materials and Methods

Figs. S1 to S15

Table S1

Materials and Methods

Materials. Lead (II) iodide (99.999%) was purchased from Sigma Aldrich. Hydrofluoric acid (40%) was purchased from Sinopharm Chemical Reagent Co., Ltd. Formamidinium iodide (FAI) (>99.5%), methylammonium iodide (>99.5%), and Spiro-OMeTAD were purchased from Advanced Election Technology Co., Ltd in China. SnO₂ colloid precursor (tin (IV) oxide, 15% in H₂O colloidal dispersion) was purchased from Alfa Aesar. Other materials were purchased from Sinopharm Chemical Reagent Co. Ltd and Sigma Aldrich and used without any further purification.

Synthesis of PEAf. A solution of 20 mmol phenethylamine in 50 mL ethanol was cooled to 0 °C in an ice bath, and 20 mmol hydrofluoric acid (40%) was added slowly with stirring. After the addition, the reaction mixture was allowed to warm to room temperature over 2 h. After removing all volatiles with a rotary evaporator, the solid was rinsed with ethyl ether, and dried under high vacuum oven overnight to afford a desired product as white powder. ¹H NMR (400 MHz, DMSO-d₆), δ (ppm): 7.66 (s, 3H), 7.25 (m, 5H), 2.98 (m, 2H), 2.92 (m, 2H). ¹³C NMR (75 MHz, DMSO-d₆), δ (ppm): 139.47, 129.09, 128.87, 126.67, 42.16, 36.90. Elemental analysis for [C₈H₁₂NF]: C, 68.02; H, 8.51; N, 9.88; Found: C, 68.06; H, 8.57; N, 9.92.

Fabrication of perovskite solar cells. ITO glass (TECA7, 7 Ω sq⁻¹, Advanced Election Technology Co., Ltd.) was cleaned by sequentially washing with detergent, deionized water, acetone, and isopropyl alcohol for 20 min, respectively, and then further treated by UVO for 15 min before use. The SnO₂ colloid precursor was diluted by DI water at volume ratio of 1:5, and spin-coated on the clean substrate at 3,000 r.p.m. for 30 s, followed by drying at 150 °C for 30 min. 1.5 M of PbI₂ in DMF:DMSO (9:1,v/v) solvent was spin-coated onto the SnO₂ at 1500 r.p.m. for 30 s, and then annealed at 70 °C for 1 min in a nitrogen glovebox. After cooling to room temperature, a solution of FAI:MAI:MACl (90 mg:6.39 mg:9 mg in 1 mL IPA) was spin-coated onto the PbI₂ film at 2,000 r.p.m. for 30 s, and then moved out and annealed at 150 °C for 15 min in ambient air conditions (30–40% humidity). For the PEAf treatment, the cooling perovskite film was exposed in a PEAf vapor environment in a closed chamber for a few seconds at 100 °C and under normal pressure, followed by annealing at 100 °C for 10 min in a nitrogen glovebox. In the cases of solution-deposition method, 20 mM PEAf (or PEAf) was dynamically coated on the perovskite film at a spin rate of 5,000 r.p.m., followed by annealing at 100 °C for 10 min in a nitrogen glovebox. On the resulting perovskite film, a HTL was deposited by spin coating a solution, which was prepared by dissolving 72.3 mg of spiro-OMeTAD, 28.8 mL 4-tert-butylpyridine, 17.5 mL of a stock solution of 520 mg mL⁻¹ lithium bis(trifluoromethylsulfonyl)imide in acetonitrile. Finally, ~ 80 nm of gold was thermally evaporated on top of the device to form the back contact.

Measurement and characterization. Current–voltage (*J–V*) characteristics were recorded by applying an external potential bias to the cell while recording the generated photocurrent with a Keithley model 2400 digital source meter. The light source was a

300 W collimated xenon lamp (Newport) calibrated with the light intensity to 100 mW cm⁻² under AM 1.5G solar light conditions by a certified silicon solar cell. The J - V curve was recorded by the forward and reverse scans with a rate of 0.1 V s⁻¹. The active areas were determined by metal shadow masks with apertures of 0.065 cm² and 1 cm². The incident photon-to-current conversion efficiency (IPCE) for solar cells was performed using a commercial setup (PV-25 DYE, JASCO). A 300 W Xenon lamp was employed as a light source for the generation of a monochromatic beam. IPCE spectra was recorded using monochromatic light without white light bias. Calibrations were performed with a standard silicon photodiode.

Device stability testing was tested for both the unencapsulated perovskite films treated with different passivators. The relative devices were conducted in a temperature-humidity chamber (DHS-100, Beijing Zhongkehuanshi Instrument Co. Ltd., China). In the experiment, the temperature was maintained at 25° C with relative humidity 45%. The photovoltaic performance of the aged devices was measured under ambient conditions.

The absorption spectra were collected using a UV-vis spectrometer (SHIMADZU, UV-1800 UV-vis Spectrophotometer) in the wavelength range of 300–900 nm. Steady-state photoluminescence (PL) was measured using Edinburgh FLS980 system with an excitation at 485 nm. Optical images of perovskite films were obtained by Nikon LV100ND optical microscope.

The powder XRD patterns and rocking curves were measured using a PANalytical Empyrean X-ray powder diffractometer equipped with a 2.2 kW Cu K α radiation (1.54 Å). For the GIXRD measurement, the incident angle was 0.1°.

The tDOS of solar cells were derived from the thermal admittance spectroscopy (TAS) method based on the frequency-dependent capacitance (C - f) measurement which were performed by an LCR meter (Agilent E4980A):^[1-3]

$$N_T(E_\omega) = -\frac{V_{bi} dC}{qWd\omega k_B T}$$

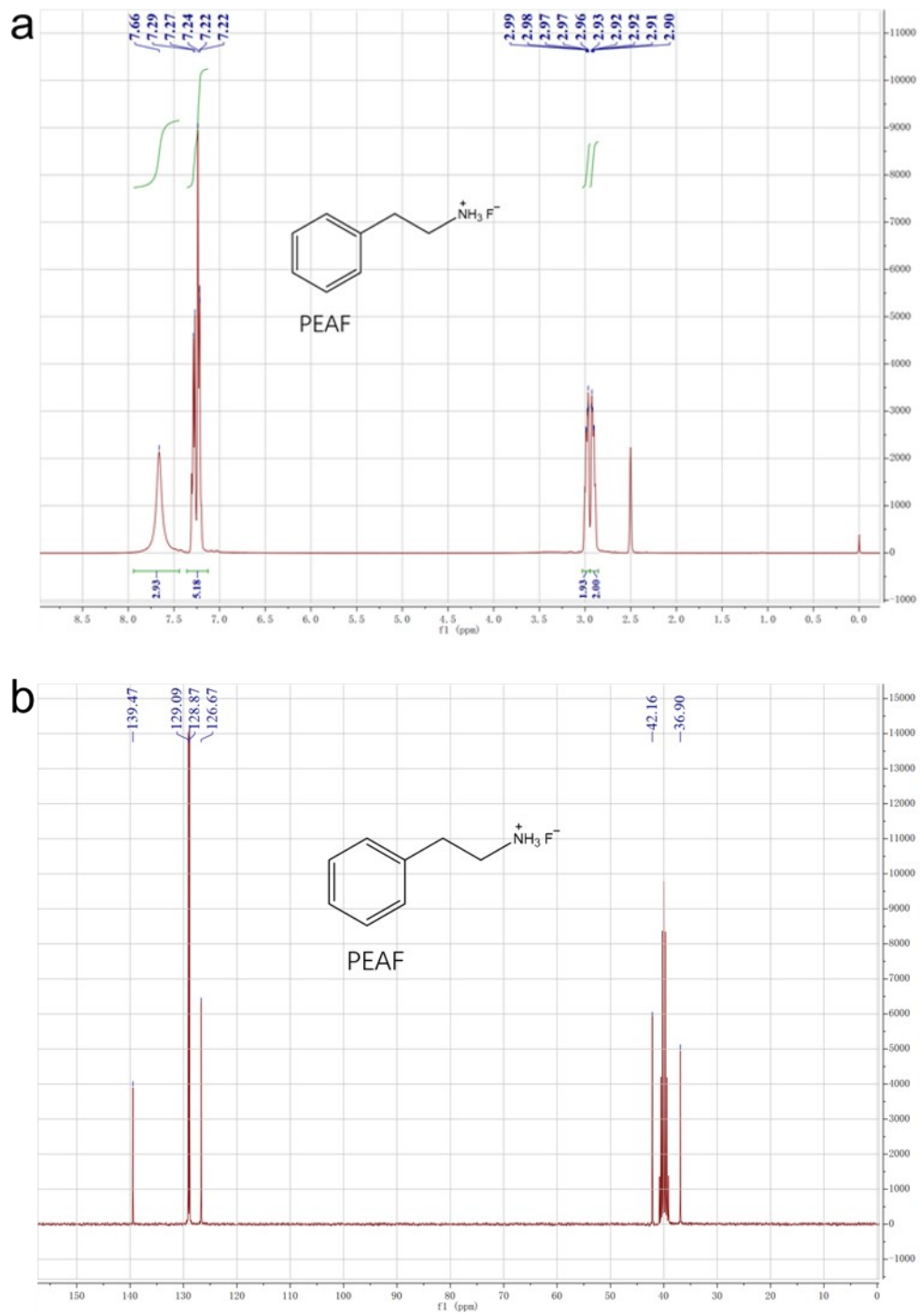
$$E_\omega = k_B T \ln\left(\frac{\omega_0}{\omega}\right)$$

where, ω is the scan angular frequency, C is the capacitance, T is the absolute temperature, W is the depletion width, V_{bi} is the built-in potential, and k_B is the Boltzmann's constant. The capacitance spectra were scanned from 0.02 kHz to 2000 kHz under dark conditions at bias voltage = 0 V at the room temperature.

The ToF-SIMS measurements were performed in a ToF-SIMS V instrument (IONTOF GmbH, Münster, Germany). During analysis, dual-beam depth profiling in an interlaced mode was used. A pulsed 30 keV Bi⁺ ion beam (10 kHz, 1.08 pA current)

was used for scanning on an area of $100 \times 100 \mu\text{m}^2$ on the sample surface. A 1 keV Cs^+ with a 68 nA beam current was used for the sputtering with a crater size of $350 \times 350 \mu\text{m}^2$. A flood gun with a current of $\approx 2 \mu\text{A}$ was used during analysis for charge compensation.

^{19}F MAS NMR spectra was measured by a Bruker AVANCE III 400 spectrometer equipped with a 2.5 mm H-F-X magic angle spinning (MAS) probe (Larmor frequency: $\nu(^{19}\text{F}) = 375.56 \text{ MHz}$). All spectra were registered using a spectrum width of 150 kHz (400 ppm), a recycle delay of 1 s, and a rotation frequency of 20 kHz or 22 kHz. All chemical shift values of ^{19}F resonances are given with respect to a KF standard (-132 ppm). ^{19}F MAS NMR spectra were collected using HPDEC (high power decoupling) pulse program.



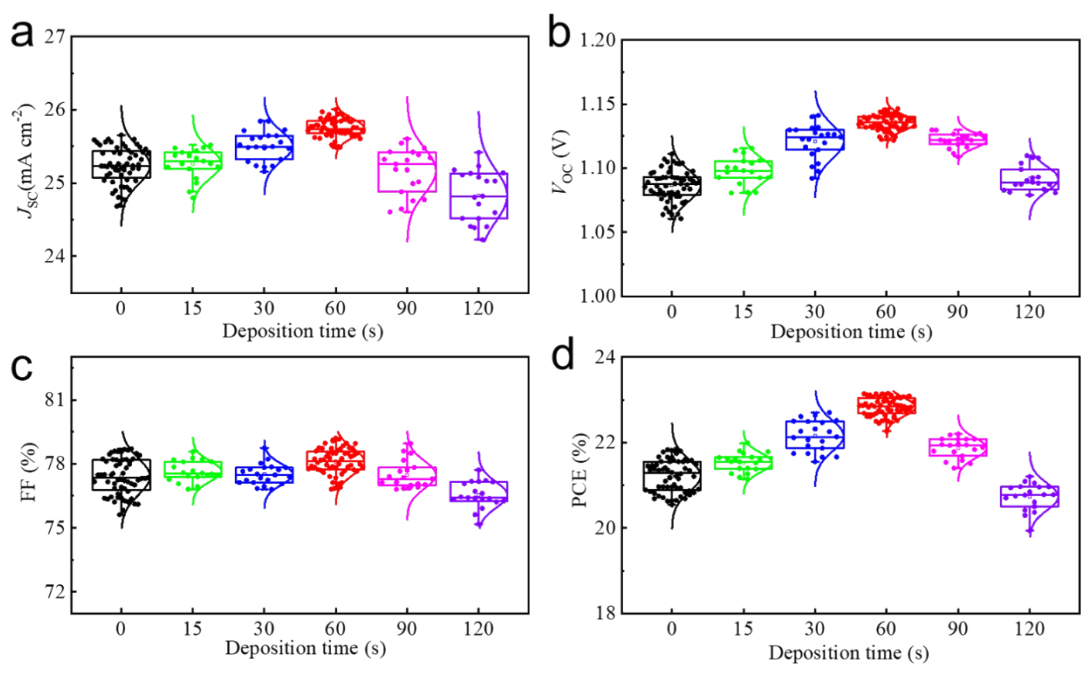


Figure S2. Statistical distributions of the photovoltaic parameters of the perovskite solar cells with the perovskite films treated by evaporated PEAf with various deposition times. Short-circuit current density (J_{sc}) (a), open-circuit voltage (V_{oc}) (b), fill factor (FF) (c), and power conversion efficiency (PCE) (d).

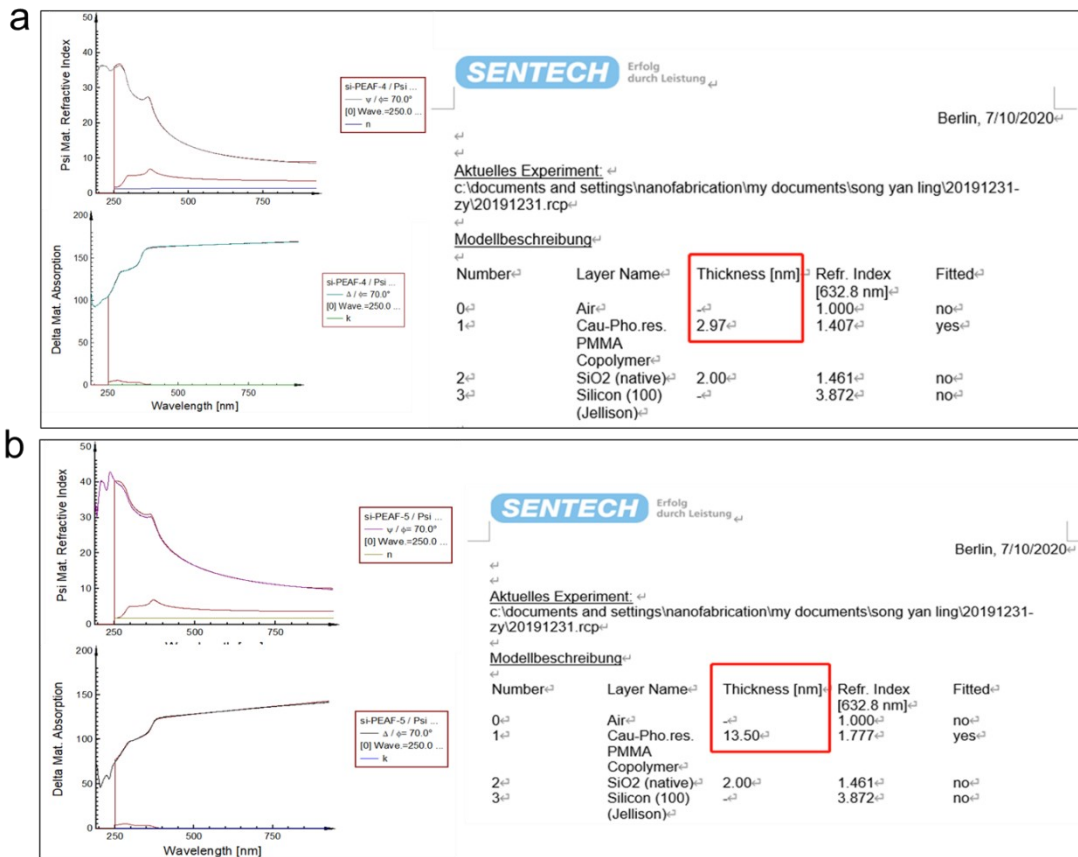


Figure S3. Thicknesses of PEAF layers on Si substrates measured by ellipsometer, where PEAI was thermally evaporated at 100 °C for 60 s in a closed chamber (a), and spin-coated with a concentration of 20 mM (b).

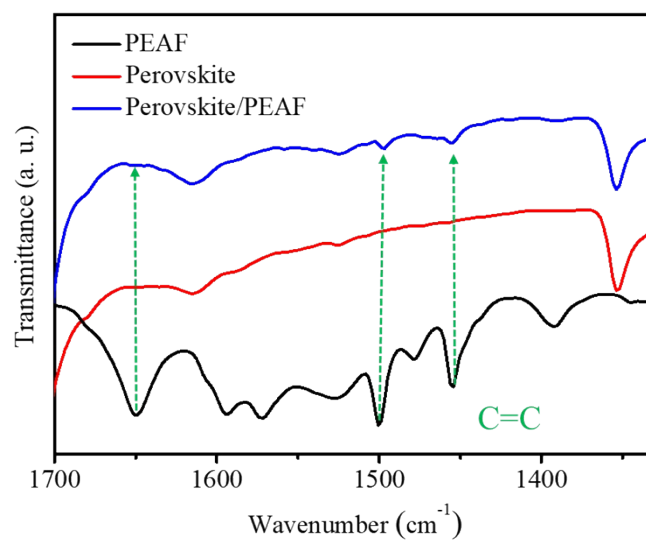


Figure S4. FTIR spectra of C=C stretch for pure PEAf, the control and PEAf-modified perovskites.

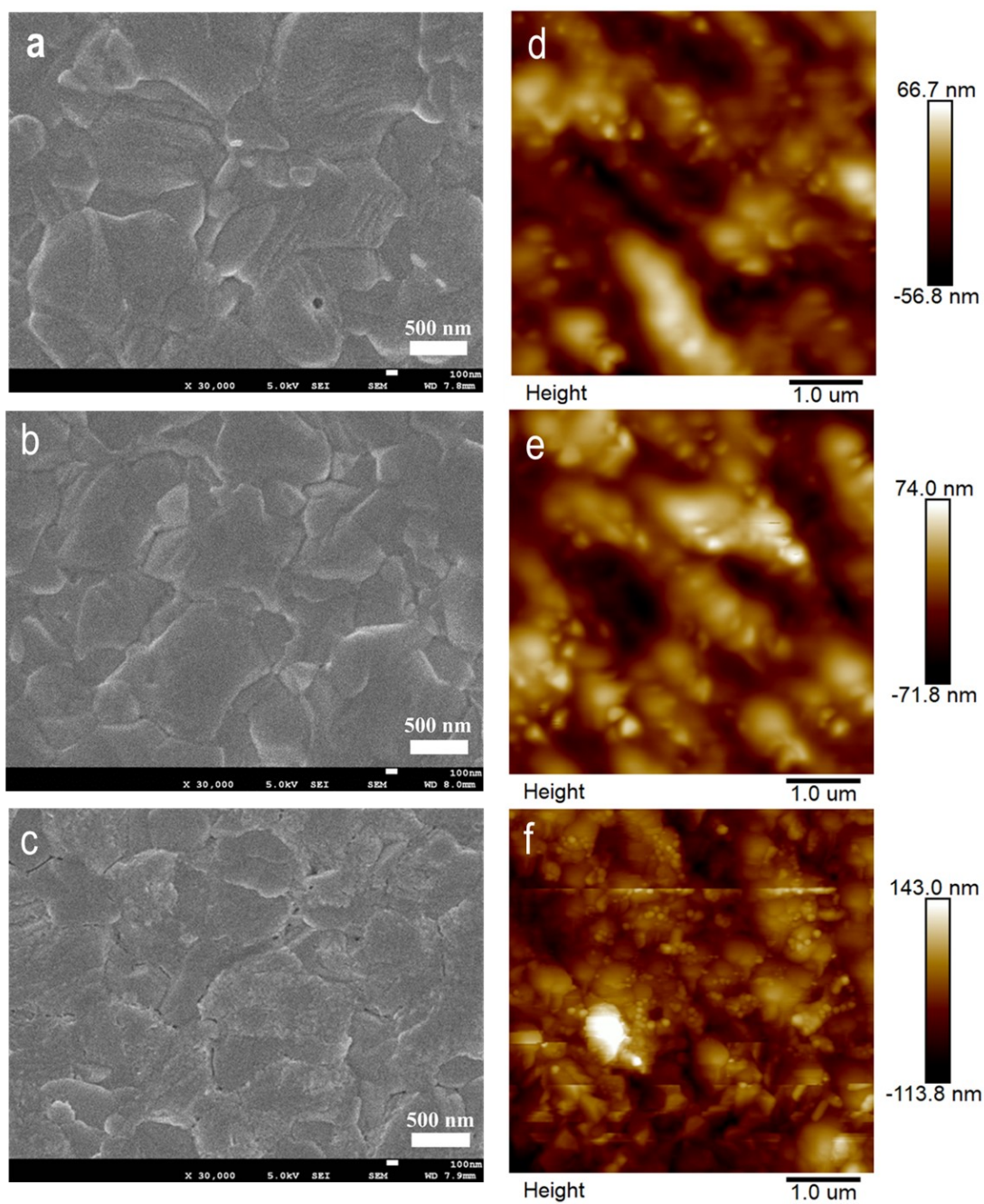


Figure S5. Top-view SEM (a, b and c) and AFM (d, e and f) images of the pristine film (a and b), and the PEA-treated perovskite films via the thermal evaporation (b and e) and solution processing (c and f) approaches, respectively.

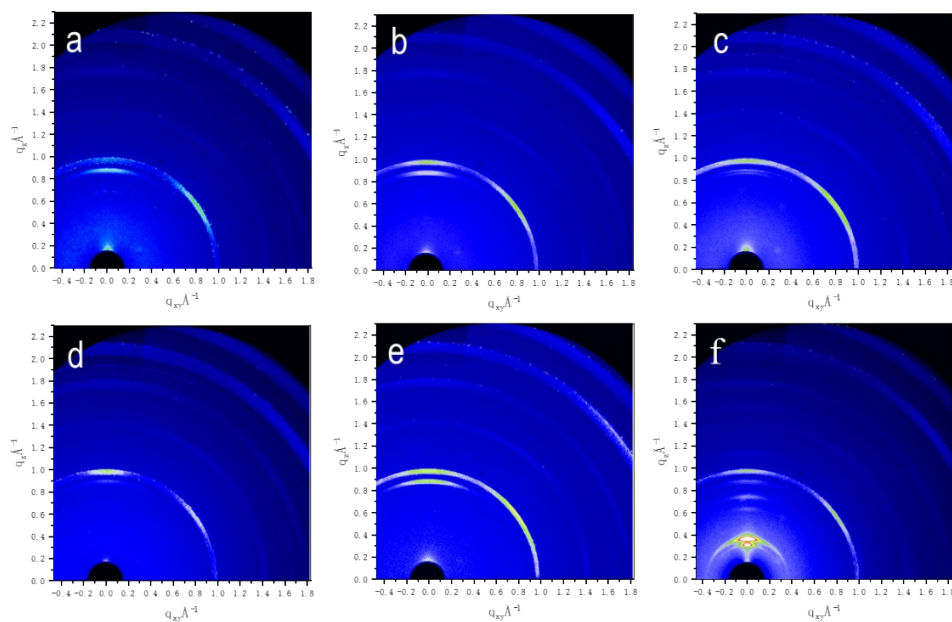


Figure S6. 2D grazing-incidence wide-angle X-ray scattering (GIWAXS) patterns of the pristine film (a), the PEAf-modified (thermal evaporation (b), solution deposited (c, 4 mM; d, 20 mM; e, 40 mM)), and PEAI-based solution deposited (f, 20 mM) perovskite films. The incidence angle is set as 0.1° .

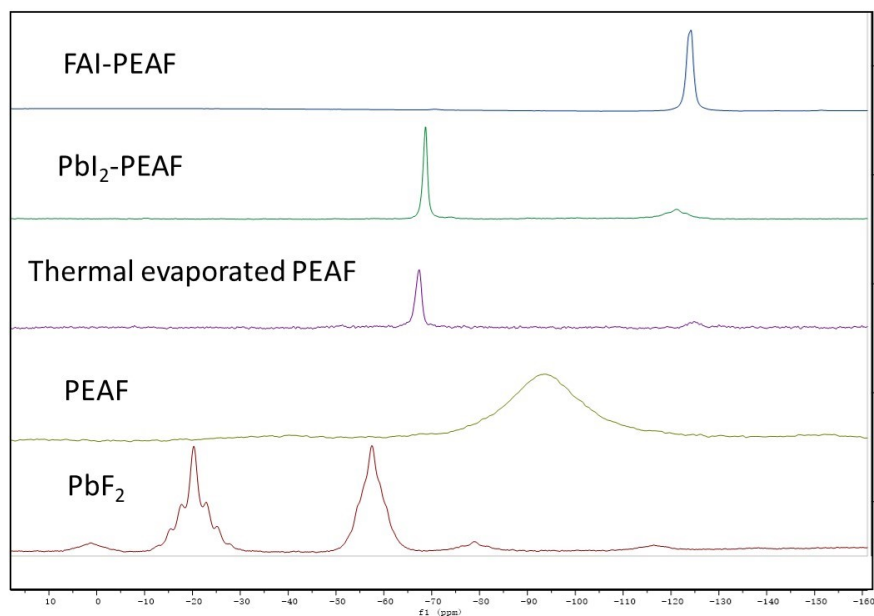


Figure S7. ^{19}F solid-state MAS NMR spectra of PEAf, PbF_2 , PbI_2 -PEAF and FAI-PEA. For the last two samples, the PEAf was mixed with the PbI_2 and FAI, respectively.

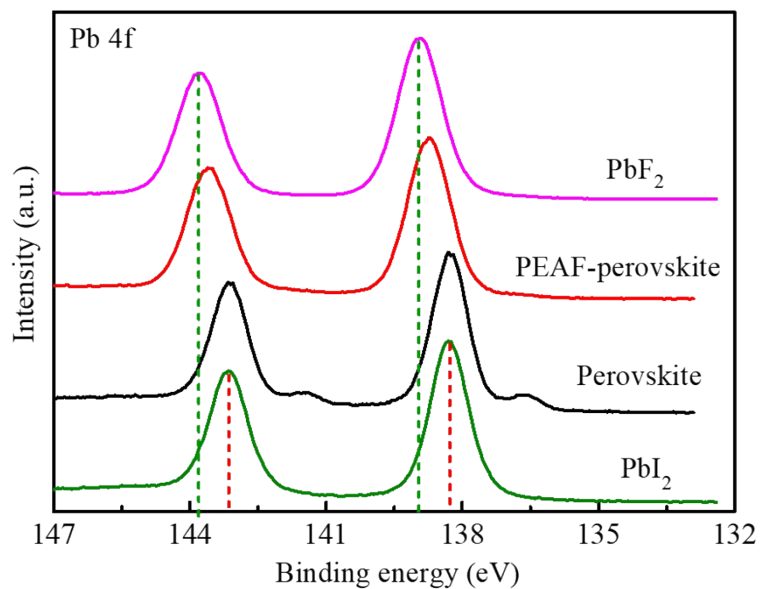


Figure S8. The spectra of Pb 4f_{7/2} and Pb 4f_{5/2} of PbF₂, PbI₂, and the perovskite films with and without the PEAf treatment.

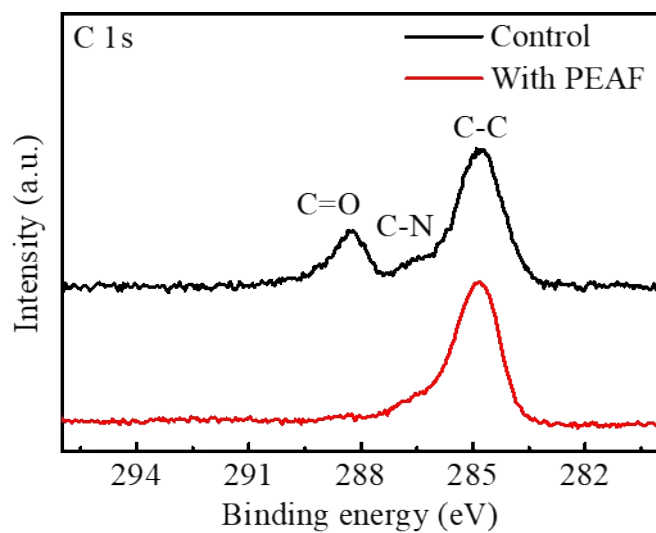


Figure S9. X-ray photoelectron spectroscopy (XPS) spectra of C 1s of the perovskite films with and without the PEAf treatment.

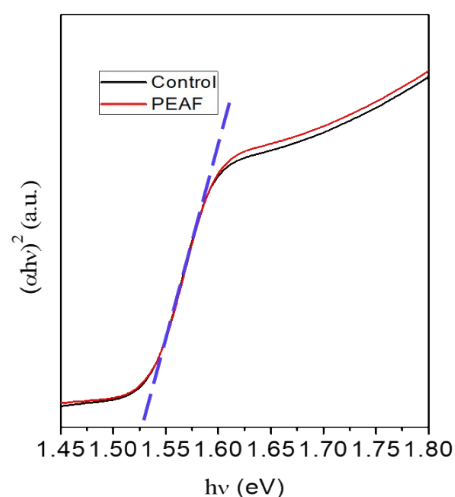


Figure S10. Tauc plots of the control and PEAf-treated perovskite film according to the corresponding absorption spectra in Figure 1d.

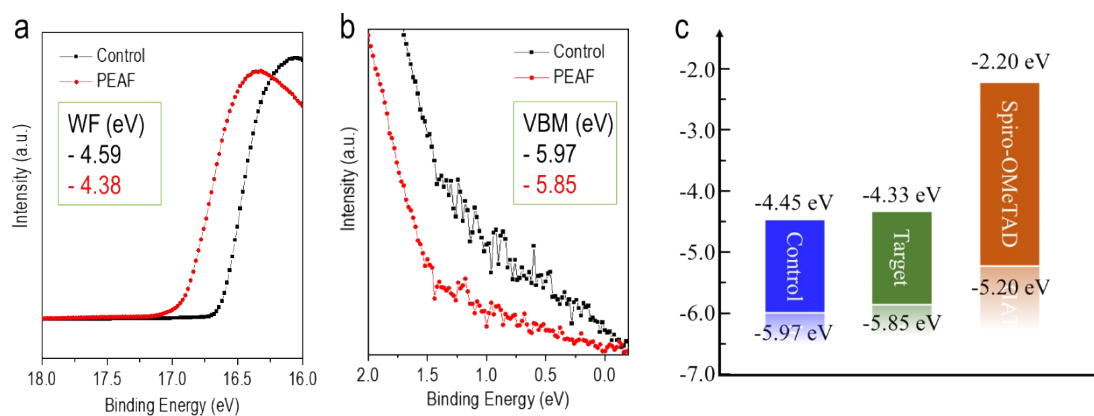


Figure S11. Ultraviolet photoelectron spectroscopy (UPS) spectra of the control and the PEAf-treated perovskite film. (a) Secondary electron cut-off region. (b) Valence band (VB) region. (c) Schematics of the energy diagram for spiro-OMeTAD, the control and PEAf-treated perovskite films. The energy band of spiro-OMeTAD was from the literature.^[4]

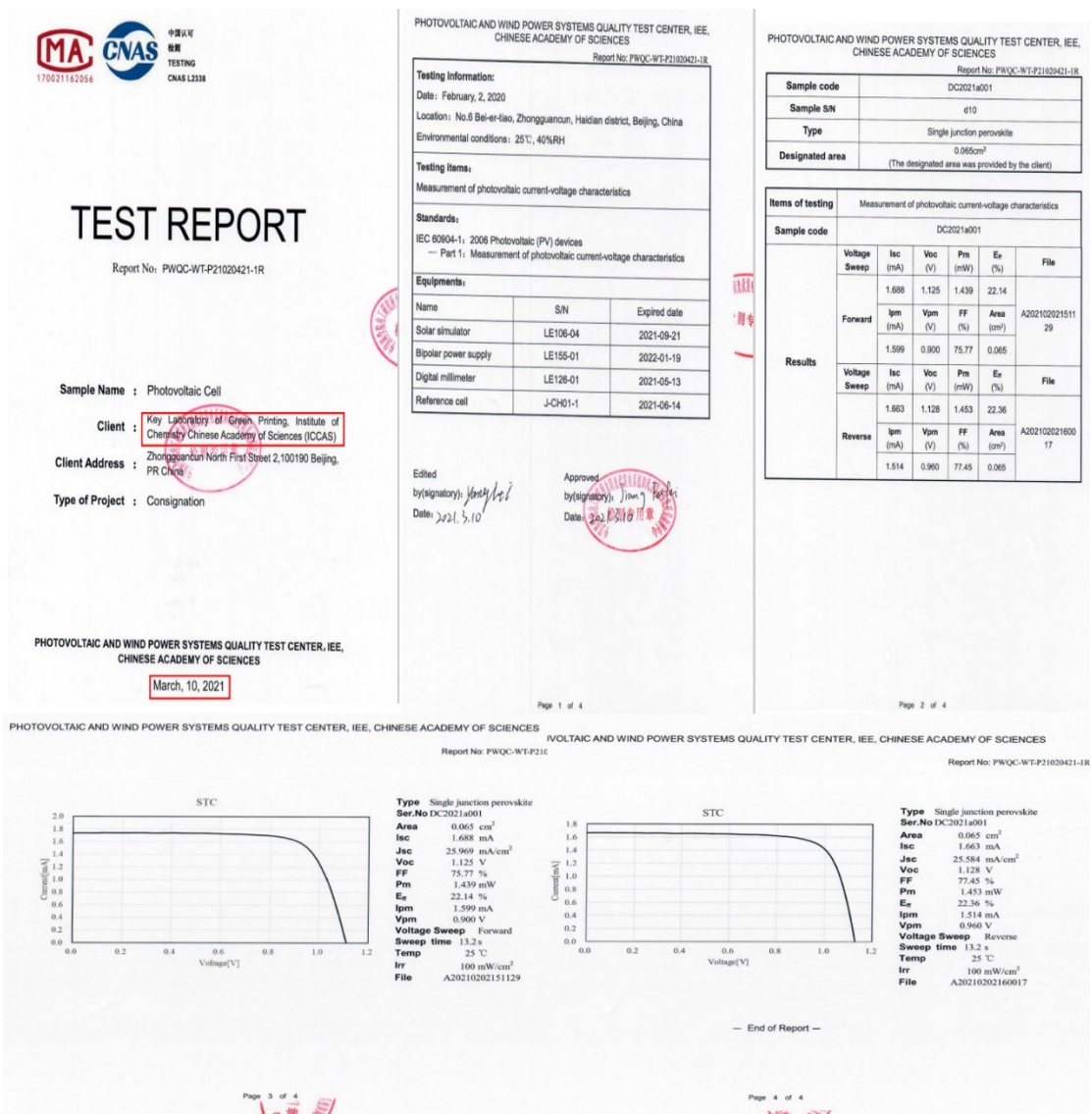


Figure S12. Certification document of the PEAf passivated perovskite solar cell (PHOTOVOLTAIC AND WIND POWER SYSTEMS QUALITY TEST CENTER CHINESE ACADEMY OF SCIENCES). The device was measured with forward scanning from 0 V to 1.2 V and reverse scanning from 1.2 V to 0 V at 100 mV s⁻¹. For the forward scanning, J_{SC} , V_{OC} and FF are 25.969 mA cm⁻², 1.125 V and 75.77%, respectively, corresponding a PCE of 22.14%, while for the reverse scanning, J_{SC} , V_{OC} and FF are 25.584 mA cm⁻², 1.128 V and 77.45%, respectively, corresponding a PCE of 22.36%. The metal mask was used with an area of 0.065 cm².

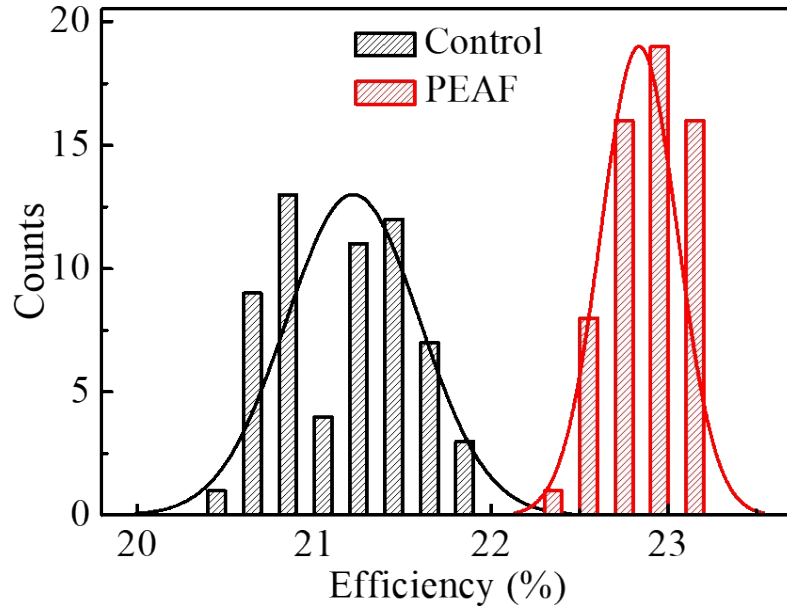


Figure S13. PCE histograms of 60 control and the PEA-treated devices measured along reverse scan directions, with the averages PCEs 21.22% and 22.84%, respectively.

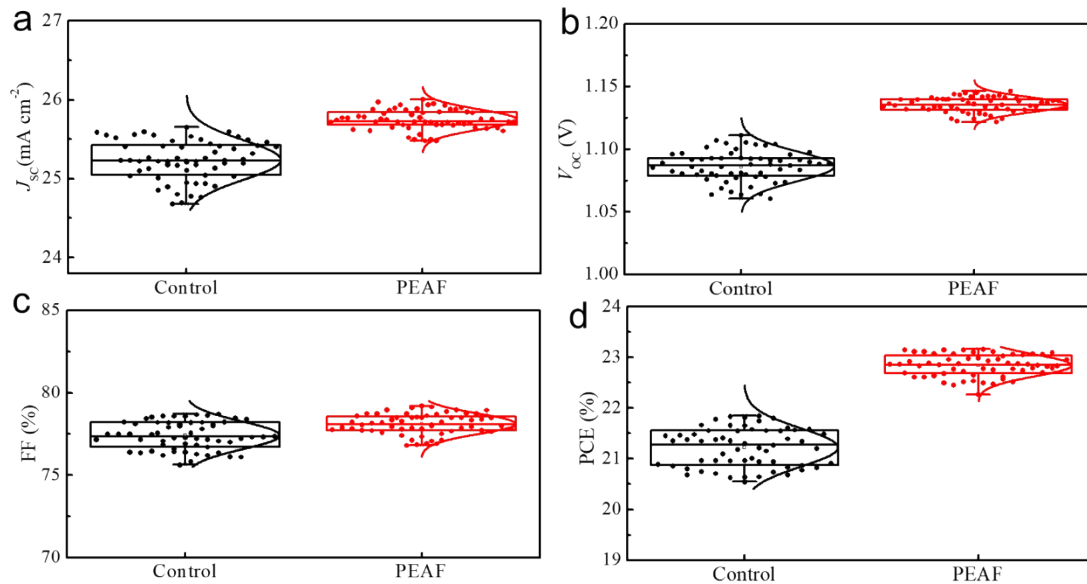


Figure S14. Statistic data showing J_{sc} , V_{oc} , FF and PCE distributions of about 60 devices obtained from control and PEA-treated PSCs.

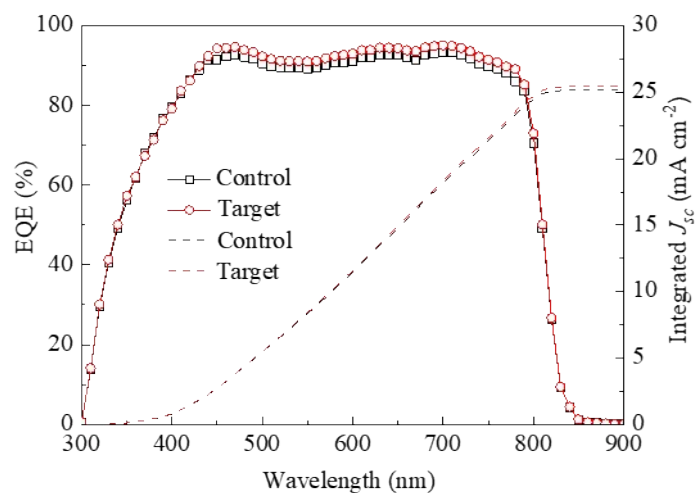


Figure S15. IPCE spectra and integrated current density of the control and target devices.

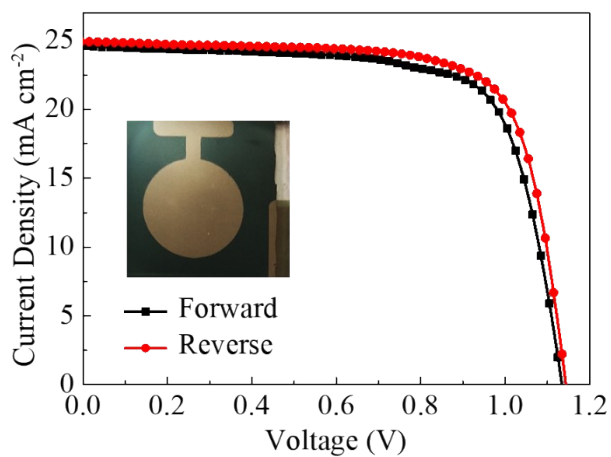


Figure S16. J - V curves of PSC with an active area of 1 cm^2 .

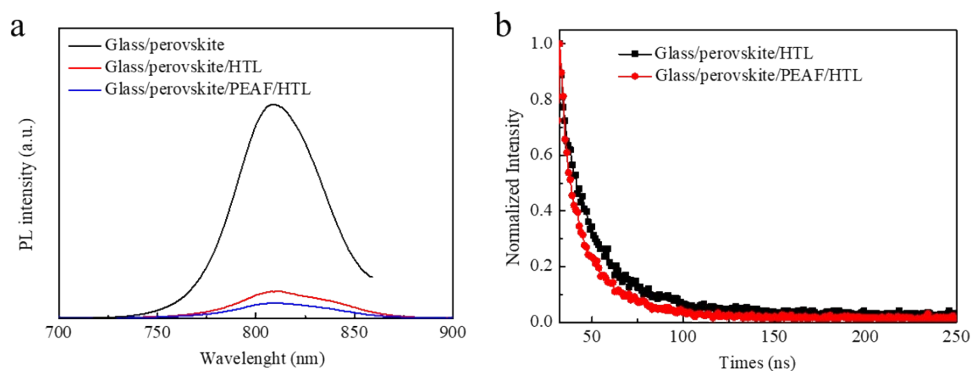


Figure S17. (a) Steady-state PL spectra of the glass/perovskite, glass/perovskite/HTL and glass/perovskite/PEAF/HTL samples. (b) TRPL spectra of the glass/perovskite/HTL and glass/perovskite/PEAF/HTL samples.



Figure S18. Images of water droplets between water and pristine (a), PEAI-treated (b) and PEAf-treated perovskite films.

Table S1: The photovoltaic parameters of the control and the PEAf-treated devices measured under forward and reverse sweeps at 0.1 V/s.

sample	style	J_{SC}	V_{OC}	FF	PCE	H-index
Control	reverse	25.52	1.107	0.773	21.84	4.90%
	forward	25.33	1.102	0.744	20.77	
PEAF	reverse	25.72	1.145	0.786	23.15	2.55%
	forward	25.51	1.141	0.775	22.56	

References

- [1] Z. Ni, C. Bao, Y. Liu, Q. Jiang, W.-Q. Wu, S. Chen, X. Dai, B. Chen, B. Hartweg, Z. Yu, Z. Holman, J. Huang, *Science* 2020, **367**, 1352–1358.
- [2] M. Samiee, S. Konduri, B. Ganapathy, R. Kottokkaran, H. A. Abbas, A. Kitahara, P. Joshi, L. Zhang, M. Noack, V. Dalal, *Appl. Phys. Lett.* 2014, **105**, 153502.
- [3] Z. Yang, Z. Yu, H. Wei, X. Xiao, Z. Ni, B. Chen, Y. Deng, S. N. Habisreutinger, X. Chen, K. Wang, J. Zhao, P. N. Rudd, J. J. Berry, M. C. Beard, J. Huang, *Nat. Commun.* 2019, **10**, 4498.
- [4] P. L. Qin, G. Yang, Z. W. Ren, S. H. Cheung, S. K. So, L. Chen, J. Hao, J. Hou, G. Li, In Situ Back-Contact Passivation Improves Photovoltage and Fill Factor in Perovskite Solar Cells. *Adv. Mater.* 2018, **30**, e1706126.